Inactivation of novel coronavirus and alpha variant by photo-renewable Cu_xO/TiO_2 nanocomposites

Tetsu Tatsuma[1,2,*], Makoto Nakakido[1], Takeshi Ichinohe[3,*], Yoshinori Kuroiwa[2], Kengo Tomioka[4], Chang Liu[4], Nobuhiro Miyamae[4], Tatsuya Onuki[1], Kouhei Tsumoto[1,3,*], Kazuhito Hashimoto[1] and Toru Wakihara[1]

[1] *School of Engineering, The University of Tokyo, 7-3-1, Hongo, Bunkyo-ku, Tokyo 113-8656, Japan*

[2] *Institute of Industrial Science, The University of Tokyo, 4-6-1 Komaba, Meguro-ku, Tokyo 153-8505, Japan*

[3] *Institute of Medical Science, The University of Tokyo, 4-6-1 Shirokanedai, Minato-ku, Tokyo 108-8639, Japan*

[4] *Nippon Paint Holdings Co., Ltd., 4-1-15 Minamishinagawa, Shinagawa-ku, Tokyo 140-8675, Japan*

Abstract

In order to reduce infection risk of novel coronavirus (SARS-CoV-2), we developed photocatalysts with nanoscale rutile TiO_2 (4–8 nm) and Cu_xO (1–2 nm or less). Their extraordinarily small size leads to high dispersity and good optical transparency, besides large active surface area. Those photocatalysts can be applied to white and translucent latex paints and a transparent varnish. Although Cu_2O clusters involved in the paint coating undergo gradual aerobic oxidation in the dark, the oxidized clusters are re-reduced under >380 nm light. The paint coating inactivated novel coronavirus and its alpha (B.1.1.7) variant under irradiation with fluorescent light for 3 h. The coating also exhibited antivirus effects on influenza A virus, feline calicivirus and bacteriophage Qβ. The photocatalysts would be applied to practical coatings and lower the risk of coronavirus infection via solid surfaces.

Introduction

Coronavirus disease 2019 (COVID-19) was first reported as a pneumonia of unknown cause in December 2019, and its pathogen was identified as a novel coronavirus (SARS-CoV-2) in January 2020. The disease caused an outbreak, and the World Health Organization (WHO) declared a pandemic in March 2020. The coronavirus is characterized by its strong infectivity. Some of the mutation variants are known to be more infectious, and were classified as variants of concern. The most majour pathway of the COVID-19 transmission is believed to be airborne aerosol including viruses from infected persons. However, there are also pathways via solid surfaces including walls, doorknobs, handrails and furniture[1]. Removal of viruses from

the surfaces would therefore reduce the risk of transmission of the disease. Photocatalyst is one of the promising materials for virus removal. A decade ago, Hashimoto and co-workers[2,3] reported that TiO_2 photocatalysts modified with Cu_xO inactivate bacteriophage Qβ. The Cu_xO/TiO_2 composites absorb visible light and electrons are excited from the TiO_2 valence band (VB) to Cu(II), and Cu(II) is reduced to Cu(I), which inactivates bacteriophage. The positive holes generated in the TiO_2 VB take electrons from ambient water, so that TiO_2 is initialized. Although Cu(I) in Cu_xO is ready to be oxidized back to Cu(II) by ambient oxygen, the Cu_xO with Cu(I) is renewed under illumination on the basis of the photocatalytic effect mentioned above.

With these mechanisms in mind, we developed novel photocatalysts that inactivate the novel coronavirus and its variant, as well as some other viruses. White and translucent paint coatings and transparent varnish coatings containing those photocatalysts were also developed. In the previous work, a rutile TiO_2 powder of 0.1–0.3 μm or larger in size was used as a typical base semiconductor material, and Cu_xO nanoparticles of ~5–8 nm diameter were deposited onto the TiO_2 powder[2,3]. Considering its large composite size and high refractive index of rutile TiO_2 of 2.5–3.0 in the visible wavelength range[4], the composite particles should tend to settle in a dispersion[5] and reflect or scatter visible light.

In the present work, we employed a sol containing rutile TiO_2 nanoparticles of ~4–8 nm in size, and deposited Cu_xO clusters of <2 nm in size to develop phtocatalysts with a high active surface area. In addition, because of the nanoscale particle size, we can fabricate translucent or transparent coatings, films and solid substrates containing the photocatalysts, which possess high designability and allow one to irradiate them both from the frontside and backside. An additional advantage of the small nanoparticles is high suspendability without sedimentation, because sedimentation velocity of nanoparticles smaller than 10–100 nm is negligibly low[5]. This is important point because only photocatalysts exposed at the coating surface are expected to affect viruses. The present sol-based wet process with nanoparticles for preparing photocatalyst coatings would allow various types of antivirus materials including paints, varnishes, gels and spray liquids to be developed. A sol containing anatase TiO_2 nanoparticles (~10 nm) was also used in the present study in place of the rutile TiO_2 sol.

Results and discussion

A rutile TiO_2 slurry (Tayca TS-310, TiO_2 diameter ~ 4–8 nm) and an anatase TiO_2 slurry (Taki Chemical M-6, TiO_2 diameter ~ 10 nm) were employed as base semiconductor materials, and aqueous solutions of $CuCl_2$, glucose as a reducing agent and NaOH were added to either of the slurries. The mol ratio of Cu to Ti was 1/20, unless otherwise noted (concentrations: 437 or 404 mM TiO_2; 62 or 57 mM glucose; 47 or 48 mM NaOH; 22 or 20 mM $CuCl_2$ for rutile and anatase, respectively). We raised its temperature to 90 °C and stirred it for 1 h to reduce Cu(II) ions to Cu(I) and deposit Cu_xO, a mixture of Cu_2O and CuO, onto TiO_2 nanoparticles. As a

result, dark suspensions were obtained. In the case of the rutile-based suspension, its colour was a greenish gray (Figure 1a), and its difference spectrum after the deposition was characterized by absorption at 400–500 nm and a broad peak at ~800 nm (Figure 1b). The latter broad peak suggests that the suspension contains excess Cu^{2+} ions. Since the former absorption band appears to be due to a semiconductor, we examined Tauc plots and obtained the band-gap values of ~3.0 and ~2.8 eV on the assumption of the direct and indirect transitions, respectively. Because Cu_2O and CuO have been reported to have direct allowed transition band-gap of 2.1–2.6 eV and indirect allowed transition band-gap of 1.2–1.6 eV, respectively[6-10], we conclude that the optical behaviour observed in the short wavelength range, from which absorption of TiO_2 has been excluded, is attributed mainly to Cu_2O. The wider band-gap in comparison with bulk Cu_2O could be due to the quantum-size effect, as discussed later.

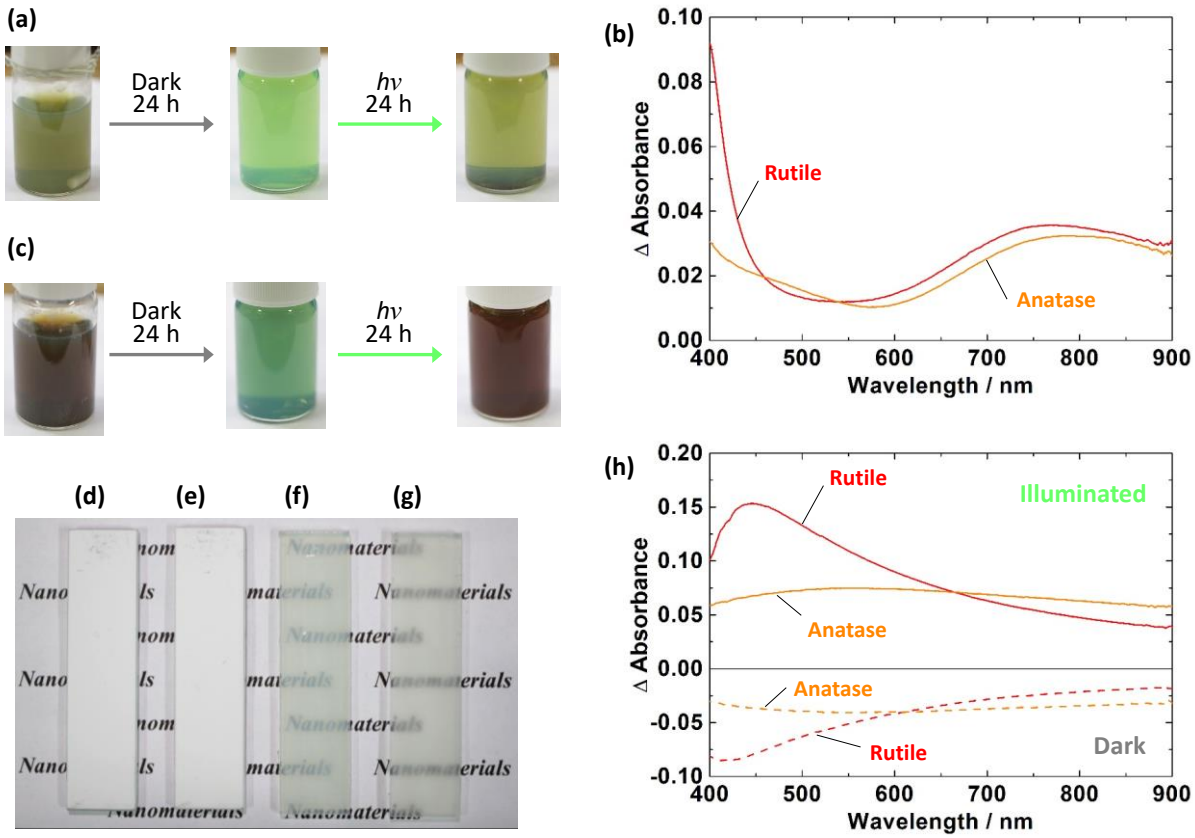

Figure 1. Colour and spectral changes of the photocatalysts. (a, c) Colour changes of the (a) rutile- and (c) anatase-based photocatalyst suspensions after leaving in the dark and under irradiation with simulated solar light. (b) Spectra of the as-prepared photocatalyst suspensions. (d–g) Photographs of the (d, f) rutile- and (e, g) anatase-based photocatalyst coating (d, e) with or (f, g) without white pigments. (h) Spectral changes of the rutile- and anatase-based coatings in the dark and under illumination (fluorescent light, >380 nm, 500 lx).

The anatase-based suspension showed a brownish gray colour (Figure 1c) and an

absorption band at 400–600 nm (Figure 1b). The corresponding Tauc plots show that the band-gap is ~2.9 eV for direct transition and ~1.7 or ~2.3 eV for indirect transition. The optical behaviour could therefore be ascribed to both Cu_2O and CuO.

We also subjected the rutile-based suspension to scanning transmission electron microscopy (STEM; JEM-ARM200F Thermal FE STEM, JEOL) and energy dispersive X-ray spectroscopy (EDS; DRY SD100GV, JEOL) after thorough evaporation of water (Figure 2). The STEM image (Figure 2a) shows that the primary size of the nanoparticles is smaller than 10 nm. As a result of elemental mapping based on STEM-EDS analysis (Figure 2d–f), we found that the majour component was TiO_2 nanoparticles of ~4–8 nm in size, and that clusters of Cu compounds (1–2 nm or less) were deposited on TiO_2. High resolution HAADF-STEM analysis proved that the TiO_2 nanoparticles were rutile phase and that the Cu compound clusters contained both Cu_2O and CuO (Figure 2b, c). The quantum-sized Cu_2O[11,12] justifies its widened band-gap of ~3.0 eV mentioned above due to a quantum-size effect.

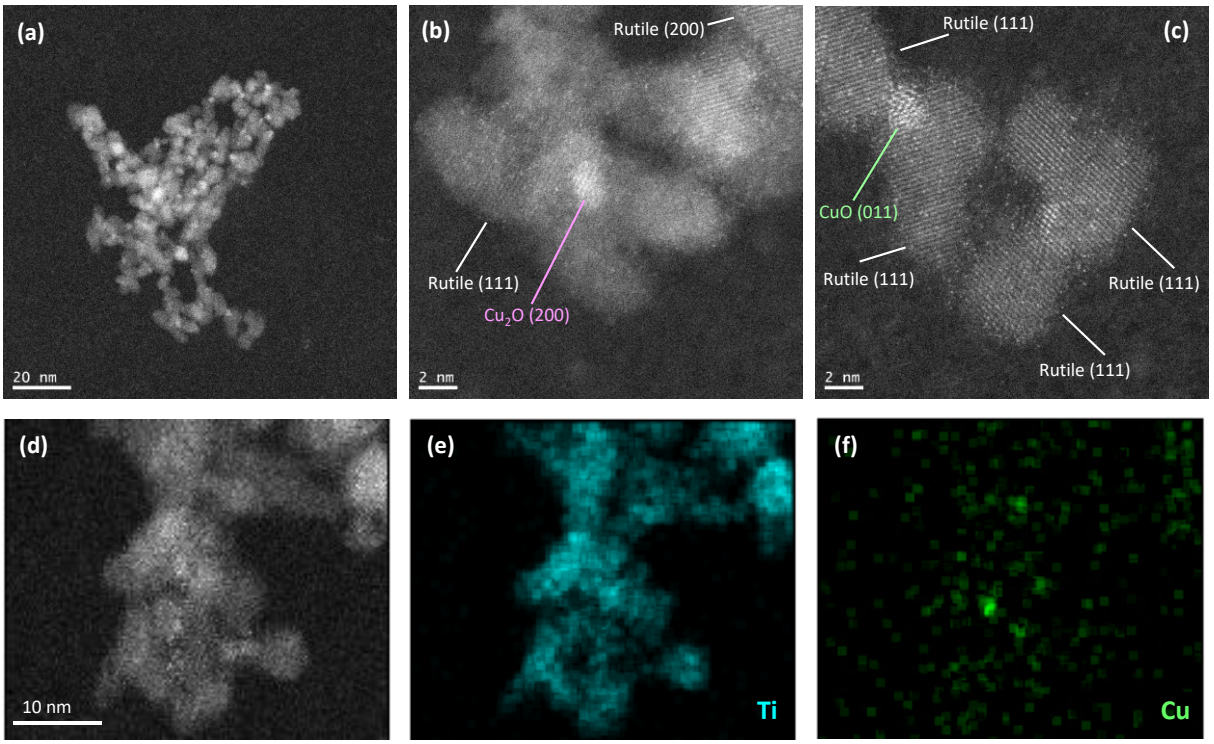

Figure 2. Photocatalyst nanoparticles. (a-d) HAADF-STEM images of the photocatalysts. (e, f) STEM-EDS elemental mapping images for (e) Ti and (f) Cu.

When the suspensions were left in the dark, their colour was gradually changed to green in 24 h (Figure 1a, c), suggesting that Cu_2O was oxidized to Cu^{2+} by dissolved oxygen (Figure 3, Process A). However, when we irradiated the oxidized suspensions with light from a solar simulator (AM1.5, ~100 mW cm^{-2}; BSS-T150, Bunko Keiki) for 24 h, their colour was changed again to greenish gray (Figure 1a) and brownish gray (Figure 1c) for rutile- and anatase-based

photocatalysts, indicating that Cu^{2+} was reduced back to Cu_2O. This reduction can be explained in terms of photo-induced interfacial charge transfer from the TiO_2 VB to Cu^{2+} at the TiO_2 surface (Figure 3, Process B).[2] Resultant holes in the TiO_2 VB should be consumed by oxidation of water to oxygen. Electrons in the TiO_2 VB could also be excited to the conduction band (CB) under the simulated solar light, which contains weak UV light, and the excited electrons could also contribute to the reduction of Cu^{2+} (Figure 3, Process C). In the case where the mol ratio of Cu to Ti was 1/100 or lower, a small absorption peak was observed at ~580 nm after irradiation of the anatase-based photocatalyst. This could be due to localized surface plasmon resonance (LSPR) of over-reduced, metallic Cu nanoparticles. Plasmonic nanoparticles in contact with TiO_2 inject electrons to the TiO_2 conduction band, and metal is oxidized to metal ions, in the case of Ag or less noble metals including Cu (Figure 3, Process D).[13,14]

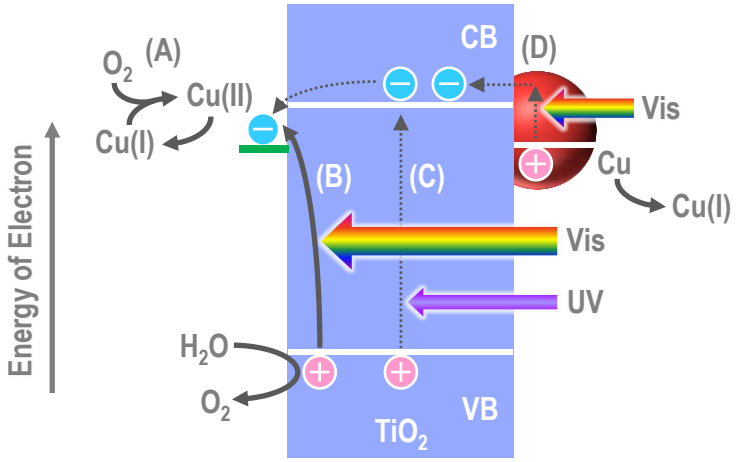

Figure 3. Photoinduced chemical processes involved in the present photo-renewable system.

Either of the Cu_xO/TiO_2 suspensions was added to a latex paint containing inorganic white pigments and organic binders, followed by 5-min stirring and 1-min degassing. Each photocatalyst slurry thus obtained was applied onto a glass plate (0.01 mL cm^{-2}). Solvent in the coating was evaporated at 25 °C for 7 days, and white films were obtained (Figure 1d, e). Colourless translucent films without the white pigment (Figure 1f, g) were also prepared for spectroscopic measurements. Their average thickness was 50 μm for both photocatalyst films. We also applied the photocatalysts to a varnish and successfully obtained transparent photocatalyst coatings. The nanoparticles were distributed almost uniformly in the transparent films, indicating that sedimentation was avoided successfully.

After preparation of the coatings, those were left in the dark. As a result, their absorption in the visible wavelength range was decreased gradually (Figure 1h). In marked contrast, the absorption was gradually increased under irradiation with fluorescent light (<380 nm light was cut off). The peak at 440 nm reflect photo-induced interfacial charge transfer from the TiO_2 VB

to Cu^{2+} [15,16]. The absorption decrease in the dark and the increase under illumination can be explained in terms of aerobic oxidation (Figure 3A) and photocatalytic re-reduction (Figure 3B), respectively, of Cu_xO clusters.

The photocatalyst paint coatings were subjected to inactivation tests against novel coronavirus (SARS-CoV-2, wild type) according to the procedures given in International Organization for Standardization ISO 21702 with some modifications. Coronaviruses in 5% FBS DMEM medium (25 μL) were applied onto a glass plate (20 × 20 mm) coated with the rutile- or anatase-based photocatalyst coating. The plate was covered with a polypropylene film of the same size and was incubated under fluorescent lamp illumination (1000 lx) for 3 h, followed by evaluation of viral infectivity V (in pfu) by a plaque assay. Figure 4a shows the log$V$ values together with those for control experiments in which a bare glass plate or a glass plate coated with the paint without photocatalyst was used instead of the photocatalytic plate. The rutile-based coating strongly inactivated the novel coronavirus and the obtained viral infectivity was lower than the detection limit of 5 pfu. Its antivirus activity [= $(\log V)_{ave} - (\log V_0)_{ave}$, where V_0 is viral infectivity for a bare glass plate and subscript ave stands for averaged values) is 3.5 or higher. The coronavirus can also be inactivated by the anatase-based coating, whereas its antivirus activity is lower (1.7). This difference should be due to the less prominent interfacial charge transfer band at 440 nm for the anatase-based photocatalyst in comparison with the rutile-based one (Figure 1h). The larger band-gap of anatase TiO_2 (3.2 eV) than rutile (3.0 eV), which lowers the contribution of the Cu^{2+} reduction pathway via the TiO_2 CB (Figure 3C), may also be responsible for the activity difference.

Next we examined an antivirus effect under illumination of the rutile-based coating on alpha variant (also known as lineage B.1.1.7 or VOC-202012/01) of the novel coronavirus, which has mutations including N501Y. We found that its antivirus activity is at least 1.5; the photocatalyst coating can inactivate alpha variant. We also subjected the photocatalyst coating to antivirus assays for other viruses by Kitasato Research Center for Environmental Science. Figure 4b shows the results for bacteriophage Qβ obtained by the protocol of Japanese Industrial Standard JIS R1756. The antivirus activities evaluated for the rutile- and anatase-based coatings were ≥5.0 and 3.4, respectively. Antivirus effects on influenza A virus and feline calicivirus, which is often used as a surrogate for norovirus because of the similarity in terms of a capsid-enveloped structure, were investigated in the dark, according to the protocol of ISO 21702. We observed significant inactivation effects of the rutile- and anatase-based photocatalyst coatings after 24-h incubation. The coatings were subjected to assay 18 days after the synthesis of the photocatalysts. We therefore conclude that Cu_2O remaining in the coating caused the antivirus effects because Cu_2O has been known to inactivate bacteriophage Qβ[17,18] and influenza virus[18].

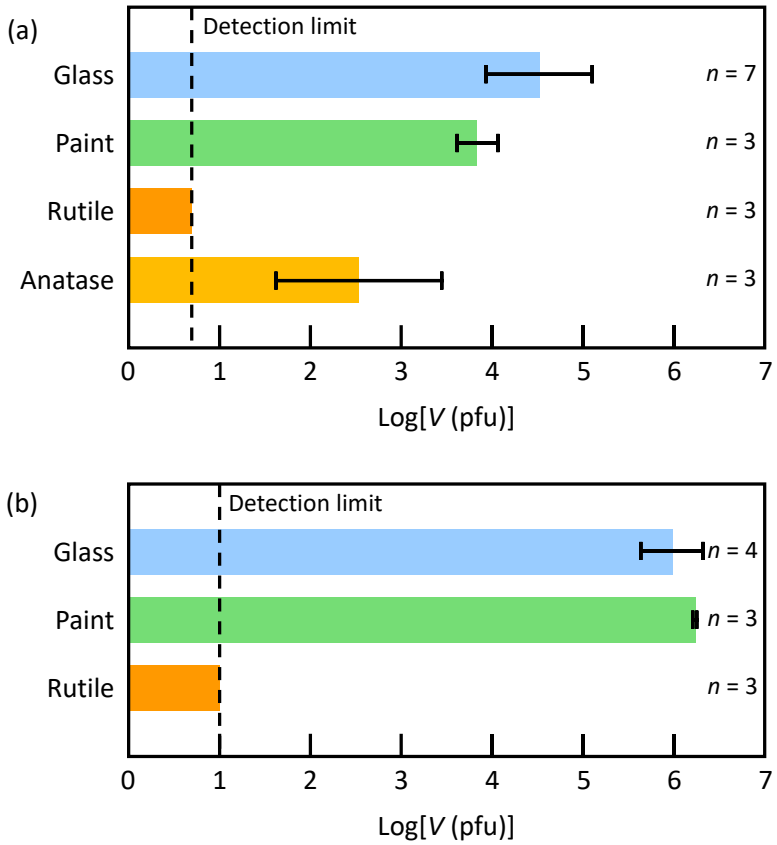

Figure 4. Antivirus effects of the rutile- and anatase-based photocatalyst coatings. The employed coatings exhibited antivirus effects on (a) the wild type novel coronavirus and (b) bacteriophage Qβ during incubation under fluorescent light (1000 lx for 3 h for coronavirus and 500 lx for 4h for bacteriophage).

Since previous studies have shown that Cu_2O inactivates influenza virus through denaturation of hemagglutinin at the virus surface[18], we investigated if the photocatalysts containing Cu_2O developed in this study denature the surface spike protein, which has a critical role in infection[19], and thereby suppress infectivity of novel coronavirus. To assess this, we prepared recombinant protein of the receptor binding domain (RBD) of spike protein and evaluated the denaturation effects of the photocatalysts on the protein. Since the binding of RBD to human ACE2, the receptor for coronavirus, is an essential step in the infection[19], the 5 μM recombinant RBD protein (70 μL) was mixed with the photocatalyst suspensions (70 μL) and left for 2 h at 4 °C and the binding activity toward ACE2 was examined by enzyme-linked immuno-sorbent assay (ELISA) according to literature[20]. As shown in Figure 5, the binding activity of RBD to ACE2 was significantly diminished by the incubation with the photocatalysts, indicating that the photocatalysts denatured the RBD protein. These results strongly support our conclusion that the antiviral effect of the photocatalyst on coronavirus relies, at least in part, on the protein denaturing activity. Further study to reveal the denaturing process of the proteins will provide a strategy to develop photocatalysts with even higher antiviral activity.

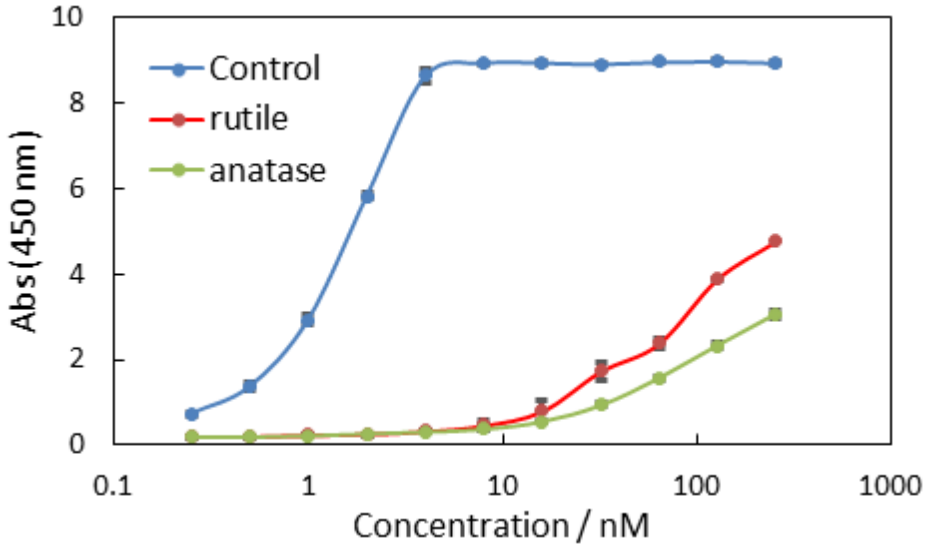

Figure 5. Denaturation effect of the rutile- and anatase-based photocatalysts on RBD domain of spike protein from coronavirus. The binding activity of RBD to human ACE2 protein at various concentrations was assessed by ELISA.

Acknowledgments

The authors are grateful to Dr. T. Ishida and Advanced Characterization Nanotechnology Platform, The University of Tokyo for HAADF-STEM and STEM-EDS measurements. Those measurements were supported in part by a Nanotechnology Platform project by the Ministry of Education, Culture, Sports, Science and Technology of Japan (No. JPMXP09A21UT0198).

References

1. N. H. L. Leung, Transmissibility and transmission of respiratory viruses. *Nature Rev. Microbiol.*, **19**, 528 (2021).
2. X. Qiu, M. Miyauchi, K. Sunada, M. Minoshima, M. Liu, Y. Lu, D. Li, Y. Shimodaira, Y. Hosogi, Y. Kuroda and K. Hashimoto, Hybrid Cu_xO/TiO_2 nanocomposites as risk-reduction materials in indoor environments. *ACS Nano*, **6**, 1609 (2012).
3. M. Liu, K. Sunada, K. Hashimoto and M. Miyauchi, Visible-light sensitive Cu(II)–TiO_2 with sustained anti-viral activity for efficient indoor environmental remediation. *J. Mater. Chem. A*, **3**, 17312 (2015).
4. J. R. Devore, Refractive indices of rutile and sphalerite. *J. Opt. Soc. Am.*, **41**, 416 (1951).
5. J. K. G. Dhont, An introduction to dynamics of colloids. Elsevier, Amsterdam, 1996.
6. J. Ghijsen, L. H. Tjeng, J. van Elp, H. Eskes, J. Westerink, G. A. Sawatzky and M. T. Czyzyk, Electronic structure of Cu_2O and CuO. *Phys. Rev. B*, **38**, 11322 (1988).
7. F. P. Koffyberg and F. A. Benko, A photoelectrochemical determination of the position of the conduction and valence band edges of p-type CuO. *J. Appl. Phys.*, **53**, 1173 (1982).
8. T. Ito, H. Yamaguchi, T. Masumi and S. Adachi, Optical properties of CuO ptudied by

spectroscopic ellipsometry. *J. Phys. Soc. Jpn.*, **67**, 3304 (1988).

9. Y. Wang, P. Miska, D. Pilloud, D. Horwat, F. Mücklich and J. F. Pierson, Transmittance enhancement and optical band gap widening of Cu_2O thin films after air annealing. *J. Appl. Phys.*, **115**, 073505 (2014).
10. Y. Wang, S. Lany, J. Ghanbaja, Y. Fagot-Revurat, Y. P. Chen, F. Soldera, D. Horwat, F. Mücklich and J. F. Pierson, Electronic structures of Cu_2O, Cu_4O_3, and CuO: A joint experimental and theoretical study. *Phys. Rev. B*, **94**, 245418 (2016).
11. A. Kellersohn, E. Knözinger, W. Langel and M. Giersig, Cu_2O quantum-dot particles prepared from nanostructured copper. *Adv. Mater.*, **7**, 652 (1995).
12. K. Borgohain, N. Murase and S. Mahamuni, Synthesis and properties of Cu_2O quantum particles. *J. Appl. Phys.*, **92**, 1292 (2002).
13. Y. Tian and T. Tatsuma, Mechanisms and applications of plasmon-induced charge separation at TiO_2 films loaded with gold nanoparticles. *J. Am. Chem. Soc.*, **127**, 7632 (2005).
14. T. Tatsuma, H. Nishi and T. Ishida, Plasmon-induced charge separation: chemistry and wide applications. *Chem. Sci.*, **8**, 3325 (2017).
15. H. Irie, S. Miura, K. Kamiya and K. Hashimoto, Efficient visible light-sensitive photocatalysts: Grafting Cu(II) ions onto TiO_2 and WO_3 photocatalysts. *Chem. Phys. Lett.*, **457**, 202 (2008).
16. H. Irie, K. Kamiya, T. Shibanuma, S. Miura, D. A. Tryk, T. Yokoyama and K. Hashimoto, Visible light-sensitive Cu(II)-grafted TiO_2 photocatalysts: activities and X-ray absorption fine structure analyses. *J. Phys. Chem. C*, **113**, 10761 (2009).
17. K. Sunada, M. Minoshima and K Hashimoto, Highly efficient antiviral and antibacterial activities of solid-state cuprous compounds. *J. Hazard. Mater.*, **235-236**, 265 (2012).
18. M. Minoshima, Y. Lu, T. Kimura, R. Nakano, H. Ishiguro, Y. Kubota, K. Hashimoto and K. Sunada, Comparison of the antiviral effect of solid-state copper and silver compounds, *J. Hazard. Mater.*, **312**, 1 (2016).
19. H. Yao, Y. Song, Y. Chen, N. Wu, J. Xu, C. Sun, J. Zhang, T. Weng, Z. Zhang, Z. Wu, L. Cheng, D. Shi, X. Lu, J. Lei, M. Crispin, Y. Shi, L. Li and S. Li, Molecular architecture of the SARS-CoV-2 virus. *Cell*, **183**, 730 (2020).
20. C. W. Tan, W. N. Chia, X. Qin, P. Liu, M. I.-C. Chen, C. Tiu, Z. Hu, V. C.-W. Chen, B. E. Young, W. R. Sia, Y.-J. Tan, R. Foo, Y. Yi, D. C. Lye, D. E. Anderson and L.-F. Wang, A SARS-CoV-2 surrogate virus neutralization test based on antibody-mediated blockage of ACE2–spike protein–protein interaction. *Nat. Biotechnol.*, **38**, 1073 (2020).